The Journal of Antibiotics (2019) 72:943–955
https://doi.org/10.1038/s41429-019-0215-7

JARA Japan Antibiotics Research Association
The Society for Actinomycetes Japan

SPECIAL FEATURE: ARTICLE

Muraminomicins, new lipo-nucleoside antibiotics from *Streptosporangium* sp. SANK 60501-structure elucidations of muraminomicins and supply of the core component for derivatization

Yoko Fujita[1] · Yoshiko Kagoshima[2] · Takeshi Masuda[3] · Masaaki Kizuka[1] · Yasumasa Ogawa[4] · Shuichi Endo[5] · Hideaki Nishigoori[5] · Kazuko Saito[6] · Kunio Takasugi[6] · Masami Miura[7] · Ryo Murakami[8] · Yasunori Muramatsu[1] · Akane Tokumitsu[9] · Tetsufumi Koga[10] · Mayumi Iizuka[1] · Azusa Aoyagi[7] · Toshihiro Suzuki[6] · Takashi Suzuki[11] · Yasuhiro Suzuki[3] · Osamu Ishida[12] · Toru Nakahira[6] · Shunichi Miyakoshi[6] · Toshiyuki Konosu[13] · Toshio Takatsu[1]

Received: 31 May 2019 / Revised: 1 July 2019 / Accepted: 3 July 2019 / Published online: 14 August 2019

Abstract

We screened for bacterial phospho-*N*-acetylmuramyl-pentapeptide-translocase (MraY: EC 2.7.8.13) inhibitors with the aim of discovering novel antibiotics and observed inhibitory activity in the culture broth of an actinomycete, SANK 60501. The active compounds, muraminomicins A, B, C, D, E_1, E_2, F, G, H, and I exhibited strong inhibitory activity against MraY with IC_{50} values of 0.0105, 0.0068, 0.0104, 0.0099, 0.0115, 0.0109, 0.0089, 0.0134, 0.0186, and 0.0094 μg ml^{-1}, respectively. Although muraminomicin F exhibited favorable antibacterial activity against drug-resistant Gram-positive bacteria, this activity was reduced with the addition of serum. To efficiently supply the core component for chemical modification studies, production was carried out in a controlled trial by adding myristic acid to the medium, and a purification method suitable for large-scale production was successfully developed.

Introduction

Since history, infectious diseases have been the main causes of death in humans. Infectious diseases that were once fatal have been cured with the advent of antibiotics, beginning with the discovery of penicillin [1]. However, in recent years, the spread of drug-resistant bacteria indicates that infectious diseases are once again emerging

Dedicated with respect to Professor K. Isono's long-standing and outstanding contribution to the isolation, structural determination, and mechanism of action of natural products, particularly nucleic acid antibiotics.

Supplementary information The online version of this article (https://doi.org/10.1038/s41429-019-0215-7) contains supplementary material, which is available to authorized users.

✉ Yoko Fujita
fujita.yoko.dx@rdn.daiichisankyo.co.jp

1 Organic Synthesis Department, Daiichi Sankyo RD Novare Co., Ltd., Tokyo, Japan

2 Medicinal Chemistry Research Laboratories, Daiichi Sankyo Co., Ltd., Tokyo, Japan

3 Biologics Technology Research Laboratories, Daiichi Sankyo Co., Ltd., Gumma, Japan

4 Daiichi Sankyo Biotech Co., Ltd., Saitama, Japan

5 Onahama Plant, Daiichi Sankyo Chemical Pharma Co., Ltd., Fukushima, Japan

6 Core Technology Research Loboratories, Sankyo Co, Ltd., Tokyo, Japan

7 Analytical & Quality Evaluation Research Laboratories, Daiichi Sankyo Co., Ltd., Kanagawa, Japan

8 Oncology Research LaboratoriesII, Daiichi Sankyo Co., Ltd., Tokyo, Japan

9 Biological Research Laboratories, Sankyo Co., Ltd., Tokyo, Japan

10 Vaccine Research Laboratories, Daiichi Sankyo Co., Ltd., Tokyo, Japan

11 Tatebayashi Plant, Daiichi Sankyo Chemical Pharma Co., Ltd., Saitama, Japan

12 Pharmaceutical Technology Laboratories, Sankyo Co., Ltd., Fukushima, Japan

13 Research Function, Daiichi Sankyo Co., Ltd., Tokyo, Japan

as a threat to human populations [2]. Conversely, the development of effective antibiotics against resistant bacteria has not been sufficient [3]. Therefore, antibiotics with novel mechanisms of action, which do not exhibit cross-resistance with conventional antibiotics, are needed. MraY is an enzyme involved in the biosynthesis of bacterial cell-wall peptidoglycans and is essential for bacterial growth. As cell wall peptidoglycans are unique to bacteria, MraY inhibitors [4] are expected to become highly selective antibacterial agents. Thus, many MraY inhibitors—liposidomycins [5], caprazamycins [6, 7], mureidomycin [8], pacidamycin [9], naspamycin [10], capuramycins [11–14], muraymycins [15], A-102395 [16], A-94964 [17, 18], and A-90289s [19]—have been reported. Although MraY inhibitors are not yet available commercially, they are believed to exhibit no cross-resistance with conventional antibiotics and thus have potential to act as a 'silver bullet'' for multidrug-resistant Gram-positive bacteria. During the course of screening for MraY inhibitors, we discovered muraminomicins from an in-house natural product library. Muraminomicins are produced by *Streptosporangium* sp. SANK 60501, and the structures are similar to those of liposidomycin and caprazamycin (Fig. 1). We previously mentioned the structures, production, purification, and MraY inhibitory activities of muraminomicins in a Japanese patent [20]. Here, we report the nuclear magnetic resonance (NMR) signal assignment and structure determination of muraminomicins and the supply of core components for their derivatization. The results of synthetic and biologic studies will be reported in subsequent paper.

Results

SANK 60501 were cultured using two 600-liter tank fermentors. The cultured broth (800 l) was subjected to various chromatography and HPLC purification steps to obtain pure muraminomicin A (**1**) 12.4, B (**2**) 13.7, C (**3**) 12.7, D (**4**) 9.0, E_1 (**5**) 10.3, E_2 (**6**) 19.0, and F (**7**) 57.7 mg (Fig. 2a).

Physico-chemical properties

The physico-chemical properties of **1**–**7** are summarized in Table S1. The molecular formula of the major component **7** was determined as $C_{55}H_{87}N_5O_{23}$ by high-resolution FAB-MS and NMR analyses. Infrared (IR) absorption of **7** implied the presence of an ester group (1738 cm^{-1}) and an amide carbonyl group (1691 cm^{-1}). The UV spectrum revealed maximum absorption at 263 nm in MeOH, which indicated the presence of uracil in **7**. A positive ninhydrin reaction suggested the presence of an amino group.

Structure determination

The structure determination of the muraminomicin F (**7**) was performed as follows, and the ^{1}H and ^{13}C NMR signal assignments of **7** are listed in Table 1. The ^{1}H NMR spectrum of **7** in DMSO-d_6 showed 80 proton resonances, and the ^{13}C NMR spectrum of **7** in DMSO-d_6 showed 55 carbon signals classified into seven methyl groups, 20 methylenes, 17 methines, 2 olefins, and 9 carbonyl carbons by the destorsionless enhancement by polarization transfer (DEPT) spectra. As these data were similar to those of liposidomycin and caprazamycin, **7** was expected to be a lipo-nucleoside compound with a diazepanone ring system.

The planar structure of **7** was determined as shown in Fig. 3a. Double-quantum filtered correlation spectroscopy (DQF-COSY), heteronuclear single-quantum coherence total correlation spectroscopy (HSQC-TOCSY), HSQC, and heteronuclear multiple bond coherence (HMBC) analysis revealed **7** to possess seven partial structures, **a**–**g**. The partial structure **c** was determined to be a diazepanone ring system by the HMBC correlations: δ_H 3.86 (H-6')/δ_C 36.4 (NCH_3), δ_H 2.26 (NCH_3)/δ_C 56.5 (C-4''') and δ_H 3.9 (H-2'''), δ_H 2.93 (NCH_3), and δ_H 3.86 (H-6')/δ_C 170.6 (C-7). The partial structures **d**, **e**, and **g** were identified as 3-hydroxymyristic acid, 3-methylglutaric acid, and succinic acid based on a gas chromatography – mass spectrometry (GC/MS) comparison study of the silylated hydrolysate of **7** with those of authentic samples and two-dimensional (2D) NMR analysis. The connectivities of seven partial structures were as follows. Based on the observed ^{1}H-^{13}C long-range couplings from δ_H 4.13 (H-3') to δ_C 77.4 (C-5') and from δ_H 3.82 (H-6') to δ_C 87.3 (C-4') in the HMBC spectrum, the partial structure **a** was connected to the diazepanone ring system **c** through C-5' oxymethine carbon. In the same way, the partial structure **b** was revealed to be linked to C-5' based upon the observed correlation between δ_H 5.38 (H-1'') and C-5'. Additionally, the partial structure **d** was located between the partial structure **c** and **e** based on the cross peaks of δ_H 5.38 (H-3''') and δ_C 169.3 (C-1a), and of δ_H 5.12 (H-3a), and δ_C 171.1 (C-1b). The connectivities of the partial structure **e**, **f**, and **g** were revealed by the observed HMBC correlations: δ_H 5.94 (H-1c)/δ_C 170.1 (C-5b), δ_H 4.97 (H-3c)/δ_C 171.8 (C-1d).

Next, we attempted to determine the relative configuration of **7** by analyzing the nuclear Overhauser effect spectroscopy (NOESY) spectrum and the ^{1}H-^{1}H and ^{13}C-^{1}H coupling constants (Fig. 3b). In the partial structure **a**, NOE correlations between H-6 and H-2'$_\beta$ (δ_H 2.0), H-3' and H-5', and H-1' and H-4' were observed. These data indicated that H-3' was β-oriented and H-4' was α-oriented. Thus, the partial structure **a** was determined to be 2-deoxyuridine (Fig. 3b). In the partial structure **b**, H-1'' and H-3'' signals

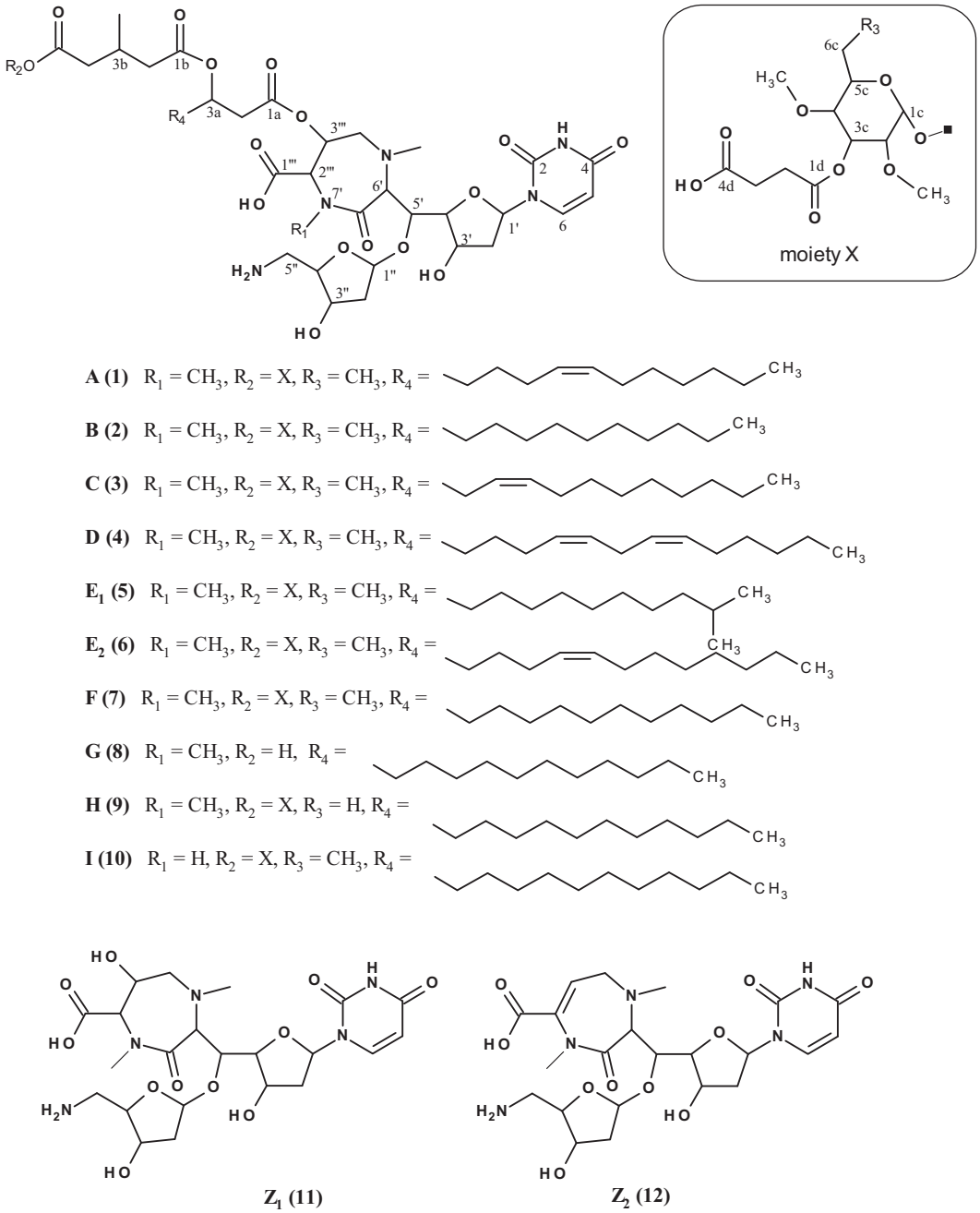

Fig. 1 Structures of muraminomicins

overlapped with those of H-3''' and H-5', respectively. To remove signal overlap, **7** was subjected to mild alkaline hydrolysis to generate deacylated derivatives named muraminomicin Z_1 (**11**) and muraminomicin Z_2 (**12**) (Fig. 1). In the ^{1}H NMR spectrum of **11**, the proton signals of H-1'' (δ_H 5.63), H-3'' (δ_H 4.46), H-4'' (δ_H 4.28), and H-5'' (δ_H 2.95 and 3.33) were observed separately. Since the correlations between H-1'' and H-4'', H-3'', and H-5'' were also observed in the NOESY spectrum of **11**, the partial structure **b** was determined to be 5-amino-2,5-dideoxy-β-ribofuranose. The stereochemistry of C-5' and the diazepanone ring system **c** could not be determined by NOE correlation analysis of **7**, **11**, and **12**. The orientations of H-3c, H-4c, and H-5c on the partial structure **f** were axial, based on the coupling constant ($J_{H\text{-}3c\text{-}H\text{-}4c} = 9.3$ Hz, $J_{H\text{-}4c\text{-}H\text{-}5c} = 9.4$ Hz). The orientation of H-2c was equatorial, based on the coupling constant ($J_{H\text{-}2c\text{-}H\text{-}3c} = 3.2$ Hz). The orientation of H-1c was equatorial based on the $^1J_{C\text{-}H}$ coupling constant ($^1J_{C1c\text{-}H1c} = 174$ Hz). Thus, the partial structure f was determined to be 6-methyl-α-rhamnose.

To date, the stereochemistry of liposidomycin and caprazamycin has been determined by various techniques

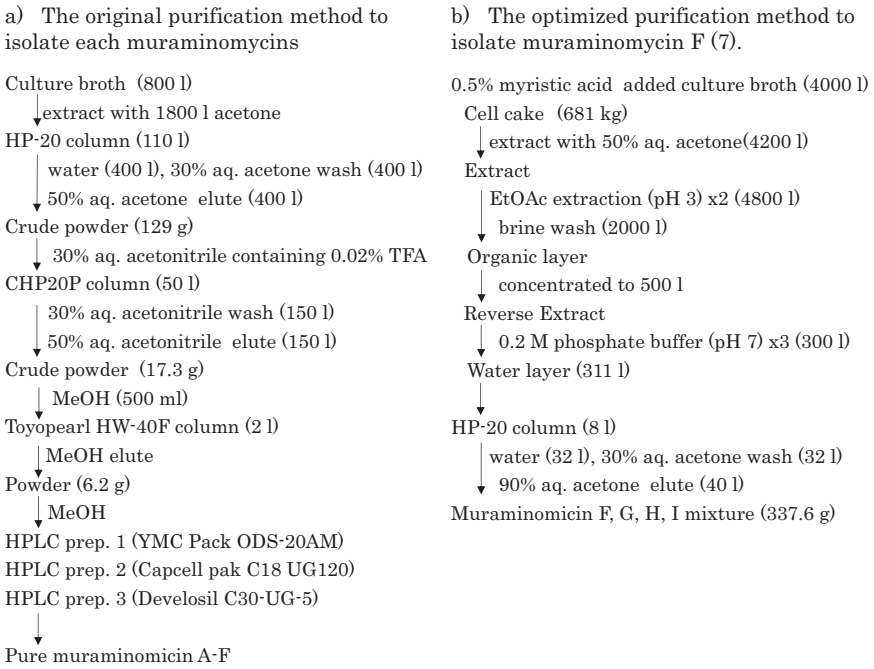

Fig. 2 Purification scheme of muraminomicins

[21–23]. We also tried to determine the stereochemistry of the core component of muraminomicin by X-ray crystallography according to the method used for caprazamycin [7]. Although we followed a reported method, we were unable to crystalize **11**. Then, we prepared *p*-bromobenzoate of **7** (**13**) and tri-*tert*-butyldimethylsilyl (TBS) derivative of **11** (**14**) both having heavy atom (Scheme S1). Although neither of these crystallized, the derivative of **11** (**15**), in which the hydroxyl groups at C-3' and C-3" were protected by TBS, was crystallized. Unfortunately, X-ray crystallographic analysis of **15** failed, because the crystal was gradually degraded by X-ray irradiation. Thus, the absolute configuration of muraminomicin core component has not been determined so far.

^{1}H and ^{13}C NMR signal assignments of **1**–**6** are listed in Tables S2–S8. The chemical shifts in the ^{1}H and ^{13}C NMR spectra of these compounds were consistent with those of **7**, except for the assignment of the fatty acid moiety; the fatty acid moieties of these compounds differed from that of **7**. Each fatty acid moiety was determined by NMR spectral analyses, including DQF-COSY, HSQC-TOCSY, HSQC, and HMBC experiments (Fig. 4).

Based on the molecular weight of **1**, and the observation of two olefinic carbon signals in the ^{13}C NMR spectrum, **1** was suggested to possess a double bond in the fatty acid moiety. Because of the substantial overlap of the olefinic protons and multiple coupled resonances of H-7a (δ_H 5.29) and H-8a (δ_H 5.33), a ^{1}H-^{1}H homodecoupling experiment was performed to clarify $J_{H\text{-}7a\text{-}H\text{-}8a}$ by irradiating the allyl methylene protons at H-6a and H-9a. The proton spin coupling constant of H-7a/H-8a could be clearly measured ($J_{H\text{-}7a\text{-}H\text{-}8a} = 10.7$ Hz) and the geometry of the double bond was determined as *cis*. The ^{13}C NMR assignments of C-7a and C-8a were determined via HSQC-TOCSY. Since the correlation between H-4a (δ_H 1.57) and δ_C 129.1 was observed more stronger than that of δ_C 130.1, the carbon signal of δ_C 129.1 was assigned to C-7a and that of δ_C 130.1 was assigned to C-8a.

The ^{1}H and ^{13}C NMR spectra of **2** were almost identical to those of **7**. Based on the molecular formula, the fatty acid moiety of **2** was determined to be 3-hydroxytridecanoic acid.

In the ^{13}C NMR spectrum of **3**, two olefinic carbon signals were observed. The DQF-COSY spectrum assigned the spin system from H-2a to H-8a, including a double bond. The proton spin coupling constant of $J_{H\text{-}5a-H\text{-}6a} = 9.8$ Hz revealed the geometry of the double bond as *cis*.

As four olefinic carbon signals were observed in the ^{13}C NMR spectrum of **4**, **4** was suggested to have two double bonds in its fatty acid moiety. To determine the geometries of the double bonds in **4**, a homodecoupling experiment was performed to measure the proton spin coupling constant, as described for **1**. Although the geometry of the double bond at 10a was determined as *cis* based on proton spin coupling constant at $J_{H\text{-}10a\text{-}H\text{-}11a} = 10.4$ Hz, another at position 7a could not be determined due to complete overlap of the H-7a and H-8a signals. To determine the geometry of the 7a position, we tried to separate the olefin and allyl methylene proton signals by changing the solvents. In the ^{1}H and ^{13}C NMR spectra of **4** dissolved in pyridine-d_5, two allyl methylene signals, H-6a (δ_H 2.19) and

Table 1 ^{1}H and ^{13}C chemical shifts of muraminomicin F (**7**) in DMSO-d_6

No.	δ_C		δ_H	No.	δ_C		δ_H
2	150.3	(s)		8a	28.9	(t)[a]	1.2–1.3 (2H, m)
4	163.3	(s)		9a	29.0	(t)[a]	1.2–1.3 (2H, m)
5	101.3	(d)	5.66 (1H, d, $J = 8.0$ Hz)	10a	29.0	(t)[a]	1.2–1.3 (2H, m)
6	140.4	(d)	7.81 (1H, d, $J = 8.0$ Hz)	11a	28.7	(t)[a]	1.2–1.3 (2H, m)
1'	84.0	(d)	5.91 (1H, t, $J = 5.9$ Hz)	12a	31.3	(t)	1.2–1.3 (2H, m)
2'	40.2	(t)	2.13 (1H, m)	13a	22.1	(t)	1.2–1.3 (2H, m)
			2.0 (1H, m)	14a	13.9	(q)	0.85 (3H, t)
3'	69.0	(d)	4.13 (1H, m)	1b	171.1	(s)	
4'	87.3	(d)	3.93 (1H, m)	2b	40.1	(t)[b]	2.35 (1H, m)
5'	77.4	(d)	4.22 (1H, m)				2.17 (1H, m)
6'	62.4	(d)	3.82 (1H, d, $J = 8.8$ Hz)	3b	27.1	(d)	2.3 (1H, m)
7'	170.7	(s)		4b	39.9	(t)[b]	2.42 (1H, dd, $J = 5.5$, 14.8 Hz)
1"	106.9	(d)	5.38 (1H, m)				2.35 (1H, m)
2"	41.4	(t)	2.0 (2H, m)	5b	170.1	(s)	
3"	70.5	(d)	4.22 (1H, m)	6b	18.9	(q)	0.93 (3H, d, $J = 6.2$ Hz)
4"	82.0	(d)	3.90 (1H, m)	1c	90.4	(d)	5.94 (1H, d, $J = 2.0$ Hz)
5"	40.5	(t)	3.0 (1H, m)	2c	76.6	(d)	3.54 (1H, m)
			2.83 (1H, m)	OCH_3	58.7	(q)	3.37 (3H, s)
1"'	169.0	(s)		3c	72.7	(d)	4.97 (1H, dd, $J = 3.2$, 9.3 Hz)
2"'	66.3	(d)	3.96 (1H, d, $J = 4.4$ Hz)	4c	77.3	(d)	3.28 (1H, dd, $J = 9.3$, 9.4 Hz)
3"'	72.8	(d)	5.38 (1H, m)	OCH_3	60.0	(q)	3.38 (3H, s)
4"'	56.6	(t)	3.4 (1H, m)	5c	74.1	(d)	3.40 (1H, m)
			3.00 (1H, m)	6c	23.9	(t)	1.71 (1H, m)
$>NCH_3$	36.3	(q)	2.28 (3H, s)				1.43 (1H, m)
$CONCH_3$	37.8	(q)	2.93 (3H, s)	7c	9.4	(q)	0.85 (3H, t)
1a	169.3	(s)		1d	171.8	(s)	
2a	38.8	(t)	2.6 (2H, m)	2d	28.9	(t)[c]	2.6 (1H, m)[d]
3a	69.9	(d)	5.12 (1H, m)				2.5 (1H, m)[d]
4a	33.3	(t)	1.56 (2H, m)	3d	29.1	(t)[c]	2.6 (1H, m)[d]
5a	24.5	(t)	1.2–1.3 (2H, m)				2.5 (1H, m)[d]
6a	28.7	(t)	1.2–1.3 (2H, m)	4d	173.5	(s)	
7a	28.9	(t)[a]	1.2–1.3 (2H, m)				

[a]Assignments may be interchanged

[b]Assignments may be interchanged

[c]Assignments may be interchanged

[d]Assignments may be interchanged

H-12a (δ_H 2.10), which overlapped in the ^{1}H NMR spectrum measured in DMSO-d_6, were observed separately. When allyl methylene H-9a (δ_H 2.92) was irradiated in a 1D NOE experiment, both the H-12a signal adjacent to *cis* olefin and another allyl methylene H-6a signal were enhanced. This indicated that the olefin at 7a position was also in the *cis* form, as observed for the 10a position. Thus, the fatty acid moiety of **4** was 3-hydroxy-(7*Z*, 10*Z*)—hexadecadienoic acid.

In the ^{1}H NMR spectrum of **5**, two equivalently resonated terminal methyl proton signals were observed as a doublet. This suggested that the fatty acid moiety of **5** had an *iso*-type terminus.

The ^{1}H and ^{13}C NMR chemical shifts of **6** resembled those of **1**. Considering the molecular formula, the alkyl chain length of the fatty acid was expected to be one-carbon longer than that of **1**. By the homodecoupling experiments irradiated H-6a and H-9a at the same time, the coupling constant between H-7a and H-8a was clearly measured as 11.0 Hz. Based on the results, the geometry of the double bond in **6** was determined to be *cis*.

Thus, the structures of **1** to **6** were determined.

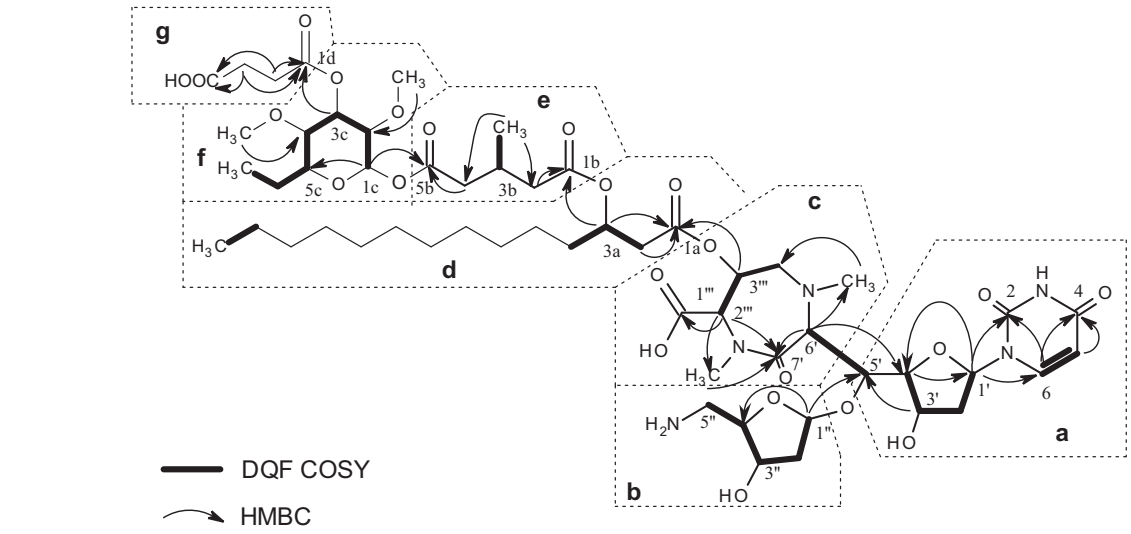

a). Planar structure of muraminomicin F (**7**) revealed by DQF-COSY and HMBC spectra in DMSO-d_6, and partial structures shown in alphabetical order

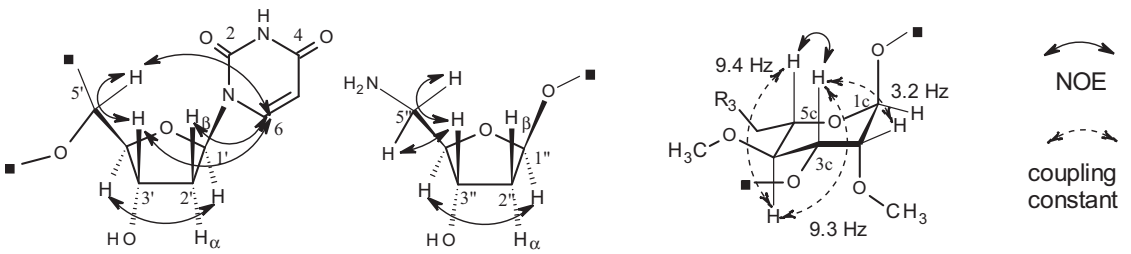

a) 2'-deoxyuridine **b**) 5-amino-2,5-dideoxyribose **f**) 2,4-di-*O*-methyl-6-methyl-α-rhamnose

b) Configuration view of 2'-deoxyuridine, 5-amino-2,5-dideoxyribose and 2,4-di-*O*-methyl-6-methyl-α-rhamnose of **7** revealed by NOESY spectrum and coupling constant

Fig. 3 NMR analysis of muraminomicin F (**7**)

Biological activity

MraY inhibitory activity of muraminomicin A–I, Z_1, and Z_2 are presented in Table 2a. Regardless of the difference in the structure of the fatty acid side chain, **1**–**10** presented potent inhibitory activities. Conversely, the inhibitory activities of **11** and **12**, in which the fatty acid moiety was eliminated, were three- to 12-times weaker than those of **1**–**7**, respectively. The antibacterial activities of **1**–**7**, **11,** and **12** are shown in Table 2b. Although the congeners **1**–**7**, which have a fatty acid side chain, exhibited favorable antibacterial activities, the deacyl derivatives **11** and **12** did not exhibit antibacterial activity. This result was consistent with the enzymatic inhibitory activity.

Next, the antibacterial spectrum of **7**, a major compound, was determined (Table 2c). Muraminomicin F (**7**) possessed excellent antibacterial activity against Gram-positive bacteria, including drug-resistant strains—methicillin-resistant *Staphylococcus aureus* (MRSA) and penicillin-resistant *Streptococcus pneumoniae* (PRSP). However, the addition of serum resulted in a making decreased in antibacterial activity. In a mouse model of systemic infection, **7** demonstrated no efficacy (data not shown). One of the reason might be caused by the effect of serum.

While **11** did not present antimicrobial activity, the strong MraY inhibitory activity was observed. Therefore, we began derivatization studies of muraminomicin in accordance with the strategy of introducing an appropriate side chain at the C-3''' position to obtain a lead compounds that show in vivo efficacy.

Production control and optimization of purification

In order to prepare of starting material for synthesis, fermentation of SANK 60501 is necessary. As various muraminomicin analogs were produced in the culture broth of SANK 60501, it was difficult to isolate each analog, and it was desirable to converge the production of various muraminomicins into one analog. As described previously, all muraminomicins can be led **11** by alkaline hydrolysis.

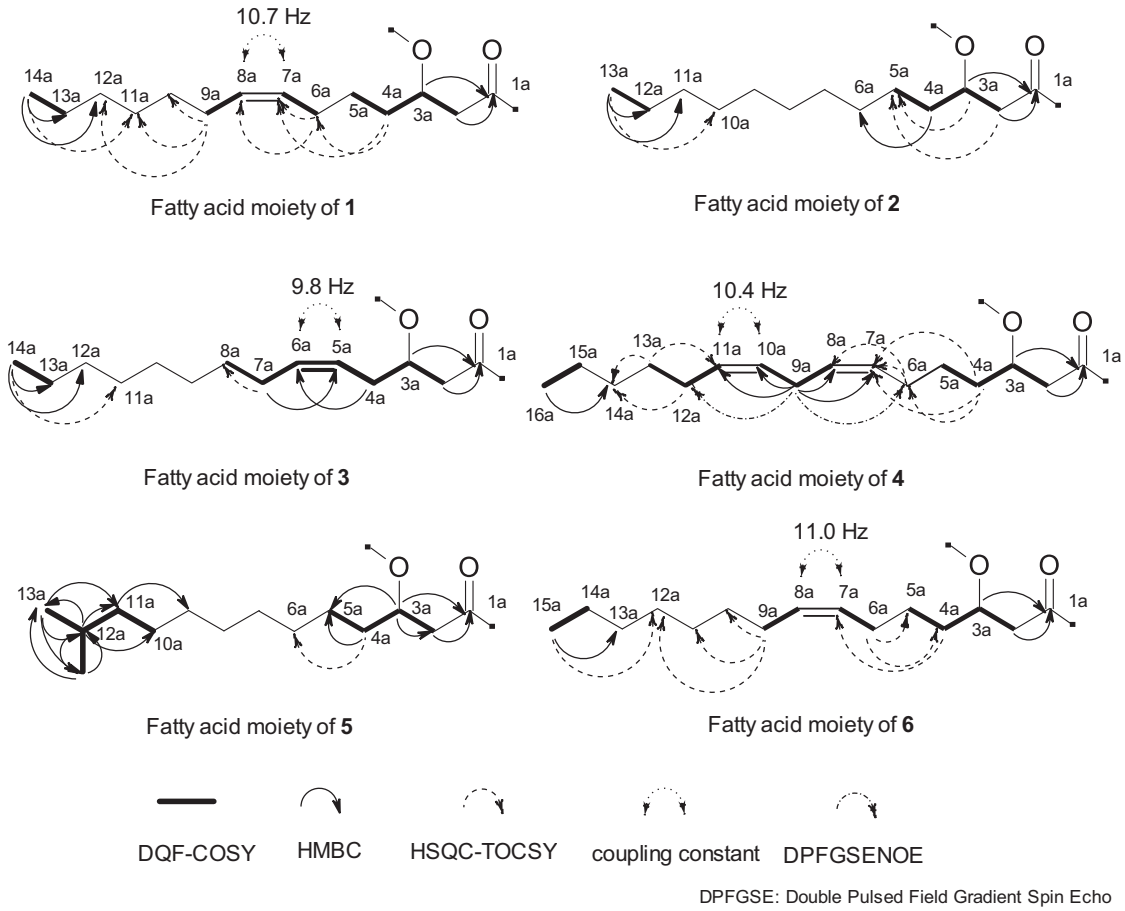

Fig. 4 NMR analysis of fatty-acid moieties in muraminomicin A (**1**) to E2 (**6**)

However, it was difficult to differentiate the substitute position of the hydroxyl group at the C-3'" from those at C-3' and C-3". Thus, a fermentation study was performed to consolidate into the product with a simple fatty acid moiety.

SANK 60501 was cultured with the addition of 0.5% myristic acid or tridecanoic acid, which were expected to be biosynthetic precursors of the fatty acid moiety of **7** and **2**. The HPLC profiles of these cultured broths are shown in Fig. S1. The production of **7** was enhanced when myristic acid, consisting of 14 carbons, was added. Similarly, the production of **2** was enhanced when tridecanoic acid, consisting of 13 carbons, was added. Thus, the fatty acid could be a precursor of the muraminomicin alkyl side chain, and the production ratio of muraminomicin side chain analogs can be controlled by the addition of fatty acid to the medium. The production of **7** was increased 2.5-fold following the addition of 0.5% myristic acid to the medium.

Next, we attempted to simplify the method of purification from the original cultured broth presented in Fig. 2a. In the original method, whole cultured broth was used for extraction. Subsequently, muraminomicins were found to accumulate in bacterial cells; therefore, extraction was performed from the mycelial cake, which was valid to reduce the following purification scale. An HP-20 column was originally used for the first step because the EtOAc extraction yield of **7** was poor. However, **7** could be extracted from the mycelial cake with 50% acetone and transferred to the organic layer by adding the same amount of EtOAc as acetone at pH 3. Furthermore, **7** could be back-extracted to the aqueous layer by phosphate buffer adjusted to pH 7. Thus, we successfully constructed an efficient method of purifying **7** without using the octadecylsilyl (ODS) column, by controlling the pH and solvent ratio (Fig. 2b). This optimization of purification improved the total yield of **7** from 32 to 67%.

HPLC analysis of the crude product obtained by this method detected three unknown analogs (Fig. S1, retention time 19.1, 31.1, and 40.5 min). These analogs were obtained in the following amounts: 17.8 mg (retention time 19.1 min [G, **8**]), 14.0 mg (retention time 31.1 min [H, **9**]), and 1.9 mg (retention time 40.5 min [I, **10**]), respectively, by various chromatography and HPLC preparation steps from muraminomicins mixture (Fig. 2b). Like other muraminomicins, the structures of **8** and **9** were determined by analyzing 2D-NMR spectral data. As for **10**, because of the low yield, the structure was confirmed by 2D-NMR and LC/

Table 2 Biological activities of muraminomicins

(a) Inhibitory activities of muraminomicins against MraY

	1	2	3	4	5	6	7	8	9	10	11	12
IC_{50} (μg ml^{-1})	0.0105	0.0068	0.0104	0.0099	0.0115	0.0109	0.0089	0.0134	0.0186	0.0094	0.0313	0.125

(b) Antibacterial activities of muraminomicin A–F, Z_1 and Z_2.

Compounds	MIC (μg ml^{-1})		
	Staphylococcus aureus 209P	*Staphylococcus aureus* 535 (MRSA)	*Enterococcus faecalis* 681
1	12.5	25	25
2	6.25	12.5	12.5
3	12.5	25	25
4	6.25	12.5	12.5
5	6.25	12.5	12.5
6	6.25	12.5	12.5
7	3.13	6.25	6.25
11	>100	>100	>100
12	>100	>100	>100

(c) Antibacterial spectrum of muraminomicin F

Test organism	MIC (μg ml^{-1})	
	Mueller-Hinton Agar	Mueller-Hinton Agar + 20% serum
Staphylococcus aureus 209P JC-1	6.25	50
Staphylococcus aureus 507 (MRSA)	6.25	50
Staphylococcus aureus 123-1 (MRSA)	6.25	50
Streptococcus pyogenes 12255	6.25	N.D
Streptococcus pneumoniae 2132 (PSSP)	6.25	N.D.
Streptococcus pneumoniae 10675 (PRSP)	3.13	N.D.
Streptococcus pneumoniae 10664 (PRSP)	12.5	N.D.
Enterococcus faecalis 10785	25	>100
Enterococcus faecium 4288	25	>100
Moraxella catarrhalis 11045	3.13	N.D
Haemophilus influenzae 11260	>100	N.D.
Escherichia coli NIHJ JC-2	>100	>100
Pseudomonas aeruginosa PAO1	>100	>100

Bacterial strains used in these studies were the standard strains (*S. aureus* 209P, *E. coli* NIHJ JC-2, *P. aeruginosa* PAO1) and the clinical isolates in Japan that were maintained in our laboratory

MS/MS analysis (Fig. S2). Although these compounds all possessed a C-14 linear fatty acid side chain, **8** had lost the 2,4-dimethoxy-3-succinyl-6-methylrhamnose moiety, **9** was the desmethyl analog of **7** at R_3, and the *N*-methyl group at R_1 was eliminated in the case of **10** (Fig. 1).

Although muraminomicin production could not be converged completely into **7**, culturing in medium containing myristic acid changed the production ratio of the components, resulting in the concentration of **7**, and small amounts of three analogs. This made it easier to monitor production by HPLC. Furthermore, we successfully simplified the purification scheme.

Discussion

To develop antibiotics without cross-resistance with conventional antibiotics, we screened for MraY inhibitors and

discovered muraminomicins, which have antimicrobial activities against Gram-positive bacteria, including MRSA and PRSP. Muraminomicins possessed a 2'-deoxyuridine moiety, a 5-amino-2,5-dideoxyribose moiety, and a diazepanone ring system. Notably, the structures of **1**–**7** differed only in their fatty acid moiety. Structure of these congeners were very similar to those of liposidomycins and caprazamycins and presented potent inhibitory activity against MraY; however, their antimicrobial activities differed. Caprazamycin B was reported to exhibit antibacterial activity against Gram-positive bacteria with the same potency as **7** [24]. Whereas non-sulfated liposidomycins, which have the same core component, have no antibacterial activity against *Staphylococcus aureus* [25]. This difference in susceptibility seems to be caused by their difference in bacterial cell membrane permeability or difference of the efficiency against drug-efflux system, which is determined by their side chain structure. Based on this hypothesis, the introduction of an appropriate acyl substituent to 3"'-OH is expected to be effective at overcoming the influence of serum and expanding the antibacterial spectrum.

By the way, a drug derivatization study originated from caprazamycins has been aspired for anti-tuberculosis drug [26], whereas we aim to develop muraminomicins as an antibiotics against Gram-positive bacteria. Caprazen derivatives, which are derived from caprazamycin, whose target enzyme is changed from MraY to WecA [27], have a double bond between C-2"' and C-3"' on the diazepanone ring, as in muraminomicin Z_2 (**12**). According to the report by Takahashi et al. [26], the caprazen derivative possessed more potent anti-tuberculous activity than caprazamycin B; however, its antibacterial activity against *S. aureus* was weaker. The MraY inhibitory activity of **12** was clearly weaker than that of **11**. Thus, the existence of the diazepanone ring structure is important for the development of an anti-Gram-positive bacterial drugs targeting MraY.

The most characteristic structural difference between muraminomicins and liposidomycins or caprazamycins was the loss of hydroxyl groups at C-2' and C-2". This difference seemed to have no influence on the MraY inhibitory activity. However, the hydroxyl groups on the C-2' and C-2" position might have the critical roles for the crystallization of core component. The stereochemistry of caprazol, the core component of caprazamycin, was revealed by X-ray crystallography, whereas **11** did not crystallize and **15** was not stable enough to apply X-ray crystallography. The reported crystalline structure of caprazol included several hydrated waters [7]. These water molecules might have key roles in crystal lattice stabilization, and the hydroxyl groups on C-2' and C-2" might be essential to maintain the hydrated water.

In conclusion, to obtain new antibiotics against Gram-positive bacteria with a novel mode of action, we fermented the producing organism, isolated muraminomicins and elucidated their structures, and succeeded in optimizing in the culture conditions to converge the product. Stereochemical studies for a better understanding of the mode of action and biosynthetic studies [28] will be continued.

Experimental procedure

General methods

Muraminomicins in the cultured broth were monitored by HPLC with a UV absorption at 260 nm on HP1100 series (Agilent Technologies, Santa-Clara, CA, USA) with a YMC Pack ODS-AM (S-3 μm, pore size 12 nm, 6.0 ϕ x 250 mm, YMC Co., Ltd., Kyoto, Japan) eluted with 53% acetonitrile water containing 0.05% TFA at a flow rate of 1.0 ml min^{-1}. The retention times of **1**, **2**, **3**, **4**, **5**, **6**, and **7** were 26.0, 28.5, 29.9, 36.2, 40.1, 40.7, and 45.1 min, respectively. All HPLC preparations during muraminomicin purification were carried out by detecting the UV absorption at 260 nm.

All NMR spectra were recorded at 300 K on an AVC 500 spectrometer (Bruker BioSpin, Kanagawa, Japan) equipped with a cryogenic probe operating at 500 MHz for ^{1}H and 125 MHz for ^{13}C NMR spectra. Optical rotation and IR spectra were measured with a DIP-370 (JASCO, Tokyo, Japan) and an FT-IR 8300 (Shimadzu, Kyoto, Japan), respectively. High-resolution ESI mass spectra were recorded on an LTQ-Orbitrap XL (Thermo Fisher Scientific, Tokyo, Japan). UV spectra were measured by a UV-265FW spectrometer (Shimadzu).

Measurement of MraY inhibitory activity

MraY inhibitory activity was measured in a 96-well microtiter polystyrene plate. The reaction was carried out in a medium as follows: 100 μl of buffer containing 100 mM Tris-HCl (pH 7.5), 50 mM KCl, 25 mM $MgCl_2$, 0.8% Triton X-100, 166 μM undecaprenyl phosphate, and 70 μM UDP-MurNAc-L-Ala-γ-D-Glu-*m*-DAP-[N^{ε}-dansyl]-D-Ala-D-Ala. The reaction was initiated by the addition of enzyme (0.625–2.5 μg protein) prepared by a method described previously [14]. Enzymatic activity was monitored by measuring the increase in emission at 538 nm (excitation at 355 nm).

Measurement of antibacterial spectrum

Minimum inhibitory concentrations (MICs) were determined by the standard agar dilution method following the Clinical Laboratory Standards Institute guideline [29]. Bacteria were incubated on Mueller-Hinton agar (Becton Dickinson) at 35 °C for 18 h. MIC measurements in mouse serum added condition were performed in the same manner except for using cation-adjusted Mueller-Hinton broth

(CAMHB, Becton Dickinson) supplemented with 50% of inactivated ddY male-mouse serum.

Taxonomy of the producing organism

The producing strain SANK 60501 was isolated from soil collected in Hokkaido Prefecture and had characteristics typical of the genus *Streptosporangium*. It developed globose sporangia at the ends of short sporangiophores on aerial mycelium. The sporangiospores were not motile. Aerial and substrate mycelium were well developed without fragmentation (Fig. S3a). A phylogenetic tree constructed using 16S rDNA sequences (1496 nucleotides) is shown in Fig. S3b. Phylogenetic analysis revealed that the SANK 60501 strain belongs to a clade of the genus *Streptosporangium*. Based on its phylogenetical and morphological properties, SANK 60501 was identified as *Streptosporangium* sp. SANK 60501 (FERM-7984).

Fermentation and isolation of muraminomicin A–F

The homogenized mycelium suspension of SANK 60501 was inoculated into seven 2-l flasks containing 500 ml of the seed medium consisting of 3% glucose, 1% yeast (Oriental Yeast Co., Ltd., Tokyo, Japan), 3% soybean powder (Nisshin OilliO, Tokyo, Japan), 0.4% $CaCO_3$, 0.2% $MgSO_4{\cdot}7H_2O$, 0.1% defoaming agent (CB442). They were cultured with shaking at 28 °C and 210 rpm for 8 days. The primary seed culture of the 5% (v/v) portion was inoculated into two 60-l jar fermentors containing 30 l of the medium mentioned above, and secondary seed culture was carried out at 28 °C and 100–200 rpm, aeration of 1 volume per volume per minute (vvm), and dissolved oxygen of 5.0 ppm for 2 days. The secondary seed culture was inoculated at 5% (v/v) into two 600-l tank fermentors containing 400 l of production medium consisting of 7% soluble starch (Kanto Chemical Co., Ltd., Tokyo, Japan), 3% pharmamedia (Archer Daniels Midland Company, IL, USA), 0.5% corn steep liquor (Oriental Yeast Co., Ltd.), 0.4% $CaCO_3$, 0.2% $MgSO_4{\cdot}7H_2O$, and 0.1% defoaming agent (CB442), and was fermented at 28 °C, with agitation at 83–200 rpm, aeration of 1 vvm, and the dissolved oxygen amount was kept 5.0 ppm for 11 days.

Eighteen-hundred-liters of acetone was added to 800 l of harvested SANK 60501 culture. After successive filtration and concentration *in vacuo*, the concentrate was added with 1400 l of water and subjected to a Diaion HP-20 column (110 l, Mitsubishi Chemical, Tokyo, Japan). The column was washed with 400 l of water and 400 l of 30% acetone in water. The active compounds were eluted with 400 l of 50% acetone in water, concentrated *in vacuo* and lyophilized to give 129 g of crude powder. This powder was dissolved with 30% acetonitrile in water containing 0.02% TFA, and subject to a CHP20P column (50 l, Mitsubishi Chemical). After the column was washed with 150 l of 30% acetonitrile in water, the active compounds were eluted with 150 l of 50% acetonitrile in water, concentrated *in vacuo* and lyophilized to give 17.3 g of crude powder. This powder was dissolved in 500 ml of methanol and applied to a Toyopearl HW-40F column (2 l, Tosoh, Tokyo, Japan). Chromatography was performed with methanol, and the eluate was fractionated into every 500-ml portion. The 8th–12th fraction was collected and concentrated *in vacuo* to give 6.2 g of powder. This powder was dissolved in 100 ml of methanol and half of the solution was subjected to a HPLC column (YMC Pack ODS-AM, 100ϕ x 500 mm, YMC Co., Ltd.) equilibrated with 45% acetonitrile in water containing 10 mM NH_4HCO_3. Chromatography was performed at a flow rate of 230 ml min^{-1}. The first fraction was eluted from the retention time 19.2–23.8 min, the second fraction was eluted from the retention time 23.8–26.8 min, and the third fraction was eluted from the retention time 26.8–30.0 min in two portions. These three fractions were separately concentrated *in vacuo* and lyophilized to give 486 mg of crude powder A from the first fraction containing **1**, **2**, and **3**, 199 mg of crude powder B from the second fraction containing **4**, **5**, and **6**, and 445 mg of crude powder C from the third fraction containing **7**.

One-hundred-milligrams of crude powder C was dissolved in 6 ml of methanol and 80 µl of the solution was subjected to a Develosil C30-UG-5 column (20ϕ x 150 mm, Nomura Chemical Co., Ltd., Aichi, Japan) equilibrated with 40% acetonitrile in water containing 10 mM NH_4HCO_3. Chromatography was performed at a flow rate of 10 ml min^{-1} and **7** was eluted at the retention time 21.1 min. The active fractions were concentrated and freeze-dried to yield 57.3 mg of **7**.

Crude powder A was dissolved in 30 ml of methanol, and 300 µl of the solution was subjected to a Capcell Pak C18 UG120 column (20ϕ x 250 mm, Osaka Soda Co., Ltd., Osaka, Japan) equilibrated with 40% acetonitrile in water containing 10 mM NH_4HCO_3. Chromatography was performed at a flow rate of 10 ml min^{-1}. The fractions eluted at retention times 21.1, 22.6, and 24.6 min were collected separately. After 100-times preparation, fractions from the same retention times were combined, concentrated *in vacuo* and lyophilized to give 25.1 mg of crude powder containing **1**, 88.0 mg of crude powder containing **2**, and 42.5 mg of crude powder containing **3**, respectively.

Crude powder B was dissolved in 15 ml of methanol, and 300 µl of the solution was subjected to a Develosil C30-UG-5 column (20ϕ x 150 mm, Nomura Chemical Co., Ltd.) equilibrated with 48.4% acetonitrile in water containing 10 mM $HCOONH_4$. Chromatography was performed at a flow rate of 10 ml min^{-1}. The fractions eluted at retention times of 19.0 and 20.1 min were collected separately. After

50-times preparation, fractions from the same retention time were combined, concentrated *in vacuo* and lyophilized to give 85 mg of crude powder containing **4** and **5**, and 29.7 mg of crude powder containing **6**, respectively. Each crude powder sample was purified by HPLC, using a Capcell Pak C18 UG120 column (20ϕ x 250 mm, Osaka Soda Co., Ltd.) or a Develosil C30 UG-5 column (20ϕ x 150 mm, Nomura Chemical Co., Ltd.). Chromatography was developed with a solvent containing $HCOONH_4$ or 10 mM NH_4HCO_3 buffer, to obtain 12.4 mg of **1**, 13.7 mg of **2**, 12.7 mg of **3**, 9.0 mg of **4**, 10.3 mg of **5**, and 19.0 mg of **6**, respectively.

Identification of 3-hydroxymyristic acid, 3-methylglutaric acid, and succinic acid

Authentic samples of 3-hydroxymyristic acid and 3-methylglutaric acid were purchased from Tokyo Chemical Industry Co., Ltd. (Tokyo, Japan) and succinic acid was purchased from FUJIFILM Wako Pure Chemical Corporation (Osaka, Japan). HCl (6 N, 500 µl) was added to each 0.5 mg of **7** and authentic samples, respectively. The solutions were sealed into the ampoule and heated at 80 °C for 15 h. After drying *in vacuo*, each hydrolyzate was dissolved in pyridine (500 µl), and added with 100 µl of *N*, *O*-bis (trimethylsilyl)trifluoroacetamide (BS-TFA, Tokyo Chemical Industry Co., Ltd.) was added at room temperature. GC/MS measurements were performed using Agilent 7890B gas chromatography coupled to a 5977A MSD (Agilent Technologies). After diluting in BSTFA, 1 µl aliquots of each sample were injected into a DB-5MS+DG capillary column (30 m length, 0.25 mm I.D., 0.25 µm Film, Agilent Technologies) in splitless mode.

Preparation and isolation of muraminomicin Z_1 (11) and Z_2 (12)

Pure powder of **7** (80 mg) was dissolved into 10 ml of 0.2 N NaOH in 50% aqueous methanol and the solution was stirred for 6 h at room temperature. The reaction mixture was adjusted to pH 7 with HCl and evaporated to remove methanol. After washing with EtOAc (5 ml) twice, the aqueous solution was freeze-dried. A mixture of the partially digested products was dissolved in 2 ml of 10 mM NH_4HCO_3 and 100 µl potion of the solution was subjected to a Capcell Pak C18 UG120 column (20ϕ x 250 mm, Osaka Soda Co., Ltd.). Column chromatography was performed with a gradient from 0 to 5% acetonitrile in water containing 10 mM NH_4HCO_3 for 23 min at a flow rate of 10 ml min^{-1}. The fractions eluted at a retention time of 15.6 and 21.9 min were collected separately 20 times. Fractions at the same retention times were combined, concentrated *in vacuo*, and lyophilized to give 11.8 mg of **11** and 5.8 mg of **12**, respectively.

Myristic acid added fermentation and isolation of muraminomicin G (8), H (9), and I (10)

A primary and secondary seed culture of SANK 60501 were performed using the same method described above. Secondary cultured broth was inoculated at 5% (v/v) into 600-liter tank fermentors containing the 300 l of medium that contained 3% glucose, 1% yeast (Oriental Yeast Co., Ltd.), 3% soybean powder (Nisshin OilliO), 0.4% $CaCO_3$, 0.2% $MgSO_4{\cdot}7H_2O$, and 0.1% defoaming agent (CB442), and cultured at 28 °C with agitation of 85 rpm, aeration of 1 vvm for 2 days. The third seed culture was inoculated with 7% (v/v) into 6000-l tank fermentors containing 4000 l of the production medium consisting of 9% soluble starch (Kanto Chemical Co., Ltd.), 3% pharmamedia (Archer Daniels Midland Company), 0.5% corn steep liquor (Orinetal Yeast Co., Ltd.), 0.5% myristic acid (Tokyo Chemical Industry Co., Ltd.), 0.25% fumaric acid (Tokyo Chemical Industry Co., Ltd.), 0.4% $CaCO_3$, 0.2% $MgSO_4{\cdot}7H_2O$, 0.1% $FeSO_4{\cdot}7H_2O$, and 0.2% defoaming agent (CB442), and fermentation was carried out at 28 °C, with agitation of 60–120 rpm, aeration of 1 vvm, and dissolved oxygen of 5.0 ppm for 11 days. During fermentation, 1000 l of water was added on the fifth day and 200 l of 30% sucrose was added on the seventh day.

Water was added to the harvested culture to make-up a total volume of 7300 l. The broth was filtered with the addition of Celite 545 (Kanto Chemical Co., Ltd.) as an adjunct. The obtained mycelial cake (681 kg) was added to 4200 l of 50% aqueous acetone and filtered again. After adjusting the pH to 3 by H_2SO_4, the filtrate (4660 l) was extracted twice with 2400 l of EtOAc. The extract (6700 l) was washed with 2000 l of brine and concentrated *in vacuo* to 500 l. The concentrate was added to 100 l of phosphate buffer (0.2 M) adjusted to pH 7 and reverse-extracted three times to the buffer layer. Half portion of the reverse extract was subjected to a Diaion HP-20 column (8 l, Mitsubishi Chemical). After the column was washed with 32 l of water and 32 l of 30% acetone in water, the active compounds were eluted with 40 l of 90% acetone in water. This method was also applied to the remaining portion and the combined active fraction was concentrated *in vacuo* to give 337.6 g of crude oil.

The crude oil was dissolved in 2 l of methanol/acetonitrile (1:1) and half of the solution was applied to a Cosmosil 140 C18 column (36 l, Nacalai Tesque Co., Ltd., Kyoto, Japan). After the column was washed with 80 l of 40% acetonitrile in water containing 0.5% of triethylamine adjusted to pH 3.4 by phosphoric acid (TEAP), chromatography was performed by stepwise elution using 45 and 50% acetonitrile in water containing the same buffer system (120

l each) and fractioned into 20-l portions. The active fractions containing **8** (40 l), **9** (20 l), or **10** (20 l) was adjusted to pH 7.

A 200-ml portion of the active fraction containing **8** was desalted by an HP-20 column (10 ml, Mitsubishi Chemical) to give 34.4 mg of crude powder. This powder was dissolved in 2 ml of methanol/acetonitrile (1:1). A 150-µl portion of the solution was subjected to a Capcell Pak C18 UG120 column (20ϕ x 250 mm, Osaka Soda Co., Ltd.) equilibrated with 48.4% acetonitrile in water containing TEAP (pH 3.3). Chromatography was performed 13 times at a flow rate of 9 ml min^{-1}, and **8** was eluted at the retention time of 21.0 min. After adjusting to pH 7, the active fraction was desalted by an HP-20 column (10 ml, Mitsubishi Chemical) and freeze-dried to yield 17.8 mg of **8** as a colorless powder.

A 60-ml portion of the active fraction containing **9** was desalted by a SepPak Plus PS-2 cartridge (1 ml, Waters, Milford, MA USA) to give 26.3 mg of crude powder. This powder was dissolved in 3 ml methanol/acetonitrile (2:1). A 250-µl portion of the solution was subjected to a Capcell Pak C18 UG120 column (20ϕ x 250 mm, Osaka Soda Co., Ltd.) equilibrated with 54.8% acetonitrile in water containing TEAP (pH 3.3). Chromatography was performed 12 times at a flow rate of 9 ml min^{-1} and **9** was eluted at a retention time of 23.9 min. After adjusting to pH 7, the active fraction was desalted by a SepPak Plus PS-2 cartridge (1 ml, Waters) and freeze-dried to yield 14.0 mg of **9** as a colorless powder.

A 600-ml portion of the active fraction containing **10** was desalted by an HP-20 column (10 ml, Mitsubishi Chemical) to give 153.2 mg of crude powder. This powder was dissolved in 2 ml of methanol/acetonitrile (1:1) and diluted by 10 mM NH_4HCO_3 water (6 ml). A 200-µl portion of the solution was subjected to a Capcell Pak C18 UG120 column (20ϕ x 250 mm, Osaka Soda Co., Ltd.) equilibrated with 42.8% acetonitrile in water containing 10 mM NH_4HCO_3. Chromatography was performed 40 times at a flow rate of 9 ml min^{-1} and **10** was eluted at a retention time of 22.5 min. The eluate was concentrated and freeze-dried to give 7.7 mg of partially purified **10**. This powder was dissolved in 600 µl of methanol/acetonitrile (1:1) and diluted in 600 µl of TEAP (pH 3.3). A 150-µl portion of the solution was subjected to a Capcell Pak C18 UG120 column (20ϕ x 250 mm, Osaka Soda Co., Ltd.) equilibrated with 54% acetonitrile in water containing TEAP (pH 3.3). Column chromatography was performed eight times at a flow rate of 9 ml min^{-1} and **10** was eluted at a retention time of 22.2 min. After adjusting the pH 7, the active fraction was desalted by a SepPak Plus PS-2 cartridge (1 ml, Waters) and freeze-dried to yield 1.9 mg of **10** as a colorless powder.

Compliance with ethical standards

Conflict of interest There is no conflict of interest from this paper publishment.

Publisher's note: Springer Nature remains neutral with regard to jurisdictional claims in published maps and institutional affiliations.

References

1. Fleming A. On the antibacterial action of cultures of a *Penicillium*, with special reference to their use in the isolation of *B. influenzae*. Br J Exp Pathol. 1929;10:226–36.
2. The evolving threat of antimicrobial resistance: options for action. Geneva, Switzerland: World Health Organization; 2012. ISBN: 9789241503181.
3. Butler MS, Blakovich MA, Cooper MA. Antibiotics in the clinical pipeline in 2013. J Antibiot. 2013;66:571–91.
4. Brandish PE, et al. Modes of action of tunicamycin, liposidomysin B and mureidomycin A: inhibition of phospho-*N*-acetylmuramyl-pentapeptide translocase from *Escherichia coli*. Antimicrob Agents Chemother. 1996;40:1640–4.
5. Ubukata M, Isosno K. The structure of liposidomycin B, an inhibitor of bacterial peptidoglycan synthesis. J Am Chem Soc. 1988;110:4416–7.
6. Igarashi M, et al. Caprazamycin B, a novel anti-tuberculosis antibiotic, from *Streptomyces* sp. J Antibiot. 2003;56:580–3.
7. Igarashi M, et al. Caprazamycins, novel lipo-nucleoside antibiotics, from *Streptomyces* sp. II. Structure elucidation of caprazamycins. J Antibiot. 2005;58:327–37.
8. Inukai M, et al. Mureidomycin A-D, novel peptidylnucleoside antibiotics with spheroplast forming activity. I. Taxonomy, fermentation, isolation and physico-chemical properties. J Antibiot. 1989;42:662–6.
9. Karwowski JP, et al. Pacidamycins, a novel series of antibiotics with anti-*Pseudomonas aeruginosa* activity. I. Taxonomy of the producing organism and fermentation. J Antibiot. 1989;42:506–11.
10. Chatterjee S, et al. Naspamycins new *Pseudomonas* active antibiotics of the mureidomycin family from *Streptomyces* sp. HIL Y-82, 11372. J Antibiot. 1994;47:595–8.
11. Yamaguchi H, et al. Capuramycin, a new nucleoside antibiotic. Taxonomy, fermentation, isolation and characterization. J Antibiot. 1986;39:1047–53.
12. Seto H, Otake N. The structure of a new nucleoside antibiotic, capuramycin. Tetrahedron Lett. 1988;29:2343–6.
13. Muramatsu Y, et al. Studies on novel bacterial translocase I inhibitors, A-500359s. I Taxonomy, fermentation, isolation, physico-chemical properties and structure elucidation of A-500359 A, C, D and G. J Antibiot. 2003;56:243–52.
14. Muramatsu Y, Ishii MM, Inukai M. Studies on novel bacterial translocase I inhibitors, A-500359s. II. Biological activities of A-500359 A, C, D and G. J Antibiot. 2003;56:253–8.
15. McDonald LA, et al. Structures of the muraymycins, novel peptidoglycan biosynthesis inhibitors. J Am Chem Soc. 2002;124:10260–1.
16. Murakami R, et al. A-102395, a new inhibitor of bacterial translocase I, produced by *Amycolatopsis* sp. SANK 60206. J Antibiot. 2007;60:690–5.
17. Murakami R, et al. A-94964, a novel inhibitor of bacterial translocase I, produced by *Streptomyces* sp. SANK 60404. I. Taxonomy, isolation and biological activity. J Antibiot. 2008;61:537–44.
18. Fujita Y, Murakami R, Muramatsu Y, Miyakoshi S, Takatsu T. A-94964, novel inhibitor of bacterial translocase I, produced by

Streptomyces sp. SANK 60404. II. Physico-chemical properties and structure elucidation. J Antibiot. 2008;61:545–9.
19. Fujita Y, et al. A-90289 A and B, new inhibitors of bacterial translocase I, produced by *Streptomyces* sp. SANK 60405. J Antibiot. 2011;64:495–501.
20. Muramatsu Y, et al. New antibiotic muraminomicin. Jpn Kokai Tokkyo Koho. 2004;JP2004-196780.
21. Knapp S, et al. Assignment of the liposidomycin diazepanone stereochemistry. J Org Chem. 2001;66:5822–31.
22. Hirano S, Ichikawa S, Matsuda A. Total synthesis of caprazol, a core structure of the caprazamycin antituberculosis antibiotics. Angew Chem Int Ed. 2005;44:1854–6.
23. Gopinath P, et al. Catalytic asymmetric total synthesis of (+)-caprazol. Org Lett. 2014;16:3364–7.
24. Igarashi M, Takeuchi T, Naganawa H, Hamada M. Antibiotic caprazamycins and process for producing the same. 2001; WO/2001/012643.
25. vKimura K, Ikeda Y, Kagami M, Yoshihama M. Selective inhibition of the bacterial peptidoglycan biosynthesis by the new type of liposidomycins. J Antibiot. 1998;51:1099–104.
26. Takahashi Y, et al. Novel semisynthetic antibiotics from caprazamycins A-G: caprazene derivatives and their antibacterial activity. J Antiobiot. 2013;66:171–8.
27. Ishizaki Y, et al. Inhibition of the first step in synthesis of the mycobacterial cell wall core, catalyzed by the GlcNAc-1-phosphate transferase WecA, by the novel caprazamycin derivative CPZEN-45. J Biol Chem. 2013;42:30309–19.
28. Chi X, et al. The muraminomicin biosynthetic gene cluster and enzymatic formation of the 2-deoxyaminoribosyl appendage. Med Chem Commun. 2013;4:239–43.
29. Clinical and Laboratory Standard Institute. Methods for dilution antimicrobial susceptibility tests for bacteria that grow aerobically. 9th ed. Approved Standard M07-A09. Wayne, PA, USA: CLSI; 2012.